AIP | Applied Physics Letters

Work function variation of MoS2 atomic layers grown with chemical vapor deposition: The effects of thickness and the adsorption of water/oxygen molecules

Jong Hun Kim, Jinhwan Lee, Jae Hyeon Kim, C. C. Hwang, Changgu Lee, and Jeong Young Park

Citation: Applied Physics Letters **106**, 251606 (2015); doi: 10.1063/1.4923202
View online: http://dx.doi.org/10.1063/1.4923202
View Table of Contents: http://scitation.aip.org/content/aip/journal/apl/106/25?ver=pdfcov
Published by the AIP Publishing

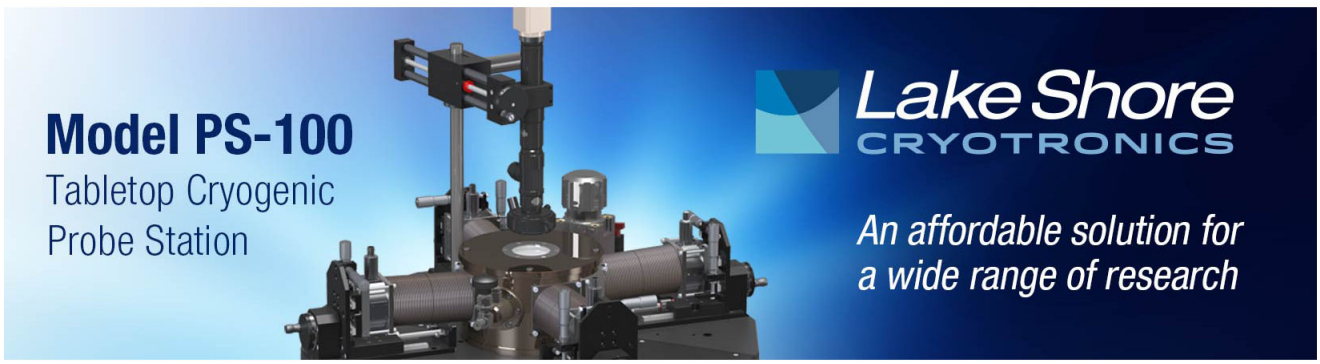

Work function variation of MoS_2 atomic layers grown with chemical vapor deposition: The effects of thickness and the adsorption of water/oxygen molecules

Jong Hun Kim,[1,2,a)] Jinhwan Lee,[3,a)] Jae Hyeon Kim,[1,2] C. C. Hwang,[4] Changgu Lee,[3,5,b)] and Jeong Young Park[1,2,b)]
[1]*Center for Nanomaterials and Chemical Reactions, Institute for Basic Science (IBS), Daejeon 305–701, South Korea*
[2]*Graduate School of EEWS, Korea Advanced Institute of Science and Technology (KAIST), Daejeon 305–701, South Korea*
[3]*School of Mechanical Engineering, Sungkyunkwan University, Suwon 440-746, South Korea*
[4]*Beamline Research Division, Pohang Accelerator Laboratory (PAL), Pohang University of Science and Technology (POSTECH), Pohang 790-784, South Korea*
[5]*SKKU Advanced Institute of Nanotechnology (SAINT) and Center for Human Interface Nano Technology (HINT), Sungkyunkwan University, Suwon 440-746, South Korea*

(Received 25 April 2015; accepted 17 June 2015; published online 26 June 2015)

The electrical properties of two-dimensional atomic sheets exhibit remarkable dependences on layer thickness and surface chemistry. Here, we investigated the variation of the work function properties of MoS_2 films prepared with chemical vapor deposition (CVD) on SiO_2 substrates with the number of film layers. Wafer-scale CVD MoS_2 films with 2, 4, and 12 layers were fabricated on SiO_2, and their properties were evaluated by using Raman and photoluminescence spectroscopies. In accordance with our X-ray photoelectron spectroscopy results, our Kelvin probe force microscopy investigation found that the surface potential of the MoS_2 films increases by ~0.15 eV when the number of layers is increased from 2 to 12. Photoemission spectroscopy (PES) with *in-situ* annealing under ultra high vacuum conditions was used to directly demonstrate that this work function shift is associated with the screening effects of oxygen or water molecules adsorbed on the film surface. After annealing, it was found with PES that the surface potential decreases by ~0.2 eV upon the removal of the adsorbed layers, which confirms that adsorbed species have a role in the variation in the work function. © *2015 AIP Publishing LLC*.
[http://dx.doi.org/10.1063/1.4923202]

The discovery of graphene opened up new prospects for technological applications in a wide range of areas. In the semiconductor industry, its excellent mobility and compatibility with existing device technologies suggested the intriguing possibility of replacing Si in field-effect transistors. However, graphene is gapless, which impedes its usage in transistor-based digital logic circuits because they require high on/off switching ratios. Instead, several transition metal-dichalcogen materials (e.g., MoS_2 and WS_2), which have sizable energy gaps, have been suggested.[1] The use of MoS_2 in switching devices is very promising: a single-layer MoS_2 transistor has been prepared with a mobility of 200 $cm^2/V{\cdot}s$ and an on/off current ratio of 10^8.[2] Various methods for the fabrication of large high-quality MoS_2 films have recently been tested, and it has been demonstrated that the chemical vapor deposition (CVD) technique is the most promising. The most frequently used approach is to evaporate sulfur gas into a pre-deposited Mo metal layer.[3,4] In another approach, MoO_3 and sulfur powder are adopted as sources.[5,6] However, it remains difficult to cover a wafer-scale area with controlled thickness and uniform mobility. Recently, Lee *et al.* successfully synthesized wafer-scale MoS_2 with high quality by performing CVD with metallic Mo and gaseous sulfur.[7] Furthermore, an array of top-gated thin film transistors consisting of 4-layer MoS_2 and a HfO_2 layer was found to exhibit a mobility of 0.12 $cm^2\ V^{-1}s^{-1}$ and an on/off current ratio of 10^5. Although various methods have been proposed,[2,8–11] to date, the performance of MoS_2 devices requires significant improvements if they are to compete with Si-based devices, which has been partially ascribed to a lack of the understanding of electrode interfaces. On a practical level, the correlation of the contact resistance with the non-ohmic barrier[12] dominates charge transport between the electrode and the channel and thus affects the overall performance; this effect can be greater for interfaces between dissimilar 2D materials.[13] Moreover, as the number of layers decreases, the charge transport and mechanical properties can change because the band structure of MoS_2 varies with thickness as a result of interlayer coupling and screening effects from impurities.[14] In this paper, we investigated the variation in the work functions of CVD-grown MoS_2 films caused by changes in thickness and the screening effects of adsorbed molecules.

The MoS_2 films were synthesized on 0.5 × 0.5 cm^2 SiO_2/Si wafer flakes; the Mo metal was pre-deposited with a precisely controlled thickness by using an e-beam evaporator. The thickness of the SiO_2 layer was ~300 nm, and the thickness of the pre-deposited Mo layer was varied from 0.5

[a)]J. H. Kim and J. Lee contributed equally to this work.
[b)]Authors to whom correspondence should be addressed. Electronic addresses: peterlee@skku.edu and jeongypark@kaist.ac.kr

to 3 nm so as to control the thickness of the resulting MoS_2 films (2 to 12 layers). After heating the Mo-deposited sample to 750 °C in a low-pressure CVD system under an Ar atmosphere, the $H_2S/H_2/Ar$ (1:5:50) reaction gas was introduced. In this process, the hydrogen gas inhibits the formation of unwanted MoO_3.[7] Raman spectra were recorded under ambient conditions by using a LabRAM HR UV-VIS-NIR Raman microscope (Horiba Jobin Yvon). The spot size was $\sim 1\ \mu m^2$, and the power was kept at 0.5 mW to prevent local heating of the samples. Ar^+ ions with an excitation energy of 2.41 eV ($\lambda_D = 514.5$ nm) were used as the laser source. For X-ray photoelectron spectroscopy (XPS) (Thermo VG Scientific Sigma Probe, Al-Kα), peak calibration was conducted with reference to the Si2*p* peak from the underlying SiO_2 film (~103.3 eV). For photoemission spectroscopy (PES), a synchrotron radiation source (the 10D beam line at the Pohang Accelerator Laboratory) was utilized.

Figure 1(a) shows the Raman spectroscopy results for the three MoS_2 samples (2, 4, and 12 layers) under ambient conditions. The two representative peaks (E^1_G and A_{1G}) near 380 and 400 cm^{-1} are clearly visible in all three spectra. The separation of these peaks decreases as the number of layers increases, as shown in Fig. 1(b). The A_{1G} mode results from the out-of-plane vibration of the S atoms, and the E^1_G mode is known to arise from the in-plane vibration of the S–Mo–S sandwich structure. As the film thickness increases, A_{1G} and E^1_G vary because of the reinforced van der Waals force and the enhanced dielectric screening, respectively.[15] The differences between the two peak frequencies are 21.5, 24.8, and 25.5 cm^{-1} for the films with 2, 4, and 12 layers, respectively. These values are consistent with those of previously reported studies.[16,17]

Kelvin probe force microscopy (KPFM) (Agilent 5500) was used to characterize the surface potential of the MoS_2 films. As KPFM can be used to quantitatively map the contact potential difference (CPD) distribution, it is now widely employed to probe the local variations in the work functions of various surfaces, such as those of 2D-materials[18,19] and nanostructures.[20] We used Pt/Ir-coated cantilevers in non-contact mode so that the topography and surface potential signal were measured simultaneously with a mechanical drive frequency of 75 kHz and an AC modulation of 1 V at 10 kHz. Tip bias was adjusted to cancel out the capacitive force generated by the work function disparity of $\phi_{tip} - \phi_{sample}$ using the equation:

$$\phi_{sample} = \phi_{tip} - e \times CPD. \quad (1)$$

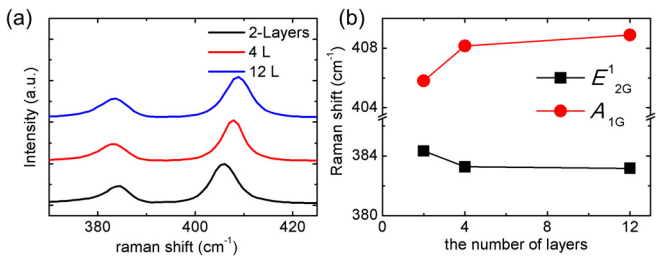

FIG. 1. (a) Raman spectra for the surfaces of MoS_2 films with thicknesses of 2, 4, and 12 layers. (b) The shifts in the peak positions for the A_{1g} and $E^1{}_{2g}$ modes as the number of layers increases from 2 to 12 layers.

Work function information can easily be obtained if ϕ_{sample} for the gold film is assumed (~5.1 eV). The work function of the probe is always calibrated in advance by scanning a gold plate, and the corresponding CPD resolution is ~50 mV, as determined by the full width at half maximum (FWHM) of the CPD histogram. Figure 2(a) shows the 400 nm × 400 nm topography and CPD images for the MoS_2 samples. The average values of the roughness were estimated from the topographical images to be 0.29, 0.24, and 0.68 nm for films with 2, 4, and 12 layers, respectively. Figure 2(a) clearly shows the layer-dependent CPD variation. Note that the CPD image contrasts are all adjusted to a common contrast intensity. As shown in the inset in Fig. 2(b), the CPD distribution of every sample is Gaussian-like regardless of either the number of layers or the small topographic artifacts that are presumed to be particles deposited during post-growth procedures Figure 2(b) shows the work functions of the samples plotted as a function of thickness using Eq. (1). The shift in the peak energy is ~0.15 eV when the number of layers is changed from 2 to 12. Considering the electron affinity (~4.3 eV) and the band gap (~ 1.3 eV) of bulk MoS_2,[21] the higher surface potentials of the thicker MoS_2 films imply that more holes are doped as the number of layers increases to 4 and 12. Although bulk MoS_2 is intrinsically an n-type semiconductor,[22,23] both n-type[2,24,25] and p-type[3,26,27] semiconductor properties have been reported for atomically thin MoS_2. According to Dolui *et al.*,[28] if the substrate is perfectly defect-free, neither charge transfer nor doping can readily occur. However, the authors suggest that if a defect arises within the interface, the activation barrier is lowered so as to produce either p-type (for Si-OH) or n-type (for Na) conducting characteristics. The latter case was ignored in our study because of the absence of Na1*s* signals in our preliminary XPS results. Note also that several recent papers have concluded that both n- and p-type conductivity regions can coexist in the same sample on a scale of tens of nanometers due to

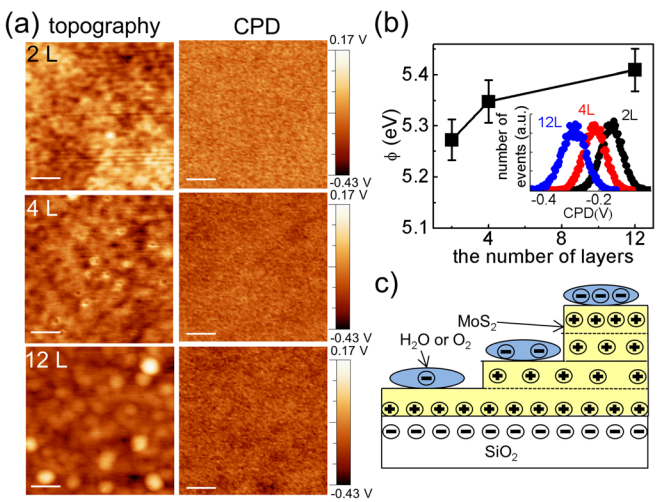

FIG. 2. (a) 400 nm × 400 nm topographical images of MoS_2 films with thicknesses of 2, 4, and 12 layers, and their corresponding contact potential maps obtained with KPFM. The scale bar is 80 nm, and the contrast for all of the surface potential images is adjusted to the same scale. (b) Work functions of the MoS_2 films as a function of layer thickness. The inset displays the work function distribution of each CPD image. (c) Schematic diagram of the MoS_2 charge distribution when O_2 or H_2O is adsorbed.

various intrinsic defect sites generated by mechanical exfoliation.[29,30] Yue *et al.*[31] reported that gas adsorption (e.g., oxygen or water) on a MoS_2 surface can modulate its Fermi level, E_F, and that adsorbed molecules act principally as charge acceptors, except for NH_3, which transfers electrons to MoS_2. However, complete screening of such charge trap centers requires the sample thickness to be thicker than a certain value that is dependent on the combination of the Thomas–Fermi screen length (λ) and the interlayer resistance.[32,33] Following Das *et al.*,[33] we assume that λ is approximately 3 nm. Thus, the thickness of a film of 12 layers marginally exceeds λ, which means that complete screening does not arise even on the topmost layer of the samples. In contrast to graphene, water or oxygen can be easily adsorbed onto MoS_2 surfaces; the extent of adsorption depends on the humidity. Adsorbed oxygen and water remove electrons from the MoS_2 film, so the increase in the work function with the number of layers can be attributed to adsorbed molecules, as indicated in Fig. 2(c).[34,35]

To evaluate the effects of doping on the variation in the work function in more detail, XPS was conducted. Figures 3(a) and 3(b) show the XPS spectra for the Mo3*d* and S2*p* core levels of each sample; the spin–orbit splitting values are 3.2 and 1.1 eV, respectively. As shown in the figures, we did not observed any considerable change in either the shape or the width. The binding energy of elemental Mo is known to be lower by ~1.2 eV than that of Mo^{4+} in MoS_2 so two Mo3$d_{5/2}$ peaks should be found unless the Mo source is fully converted to MoS_2.[29,36] To determine the chemical compositions of the samples, the Mo3*d* and S2*p* peak areas were utilized with relative sensitivity factors of 9.5 and 1.67, respectively. The chemical ratio was ~2.1, and this value was found to be not significantly affected by the variation of the film thickness. According to McDonnell *et al.*,[29] the S/Mo ratio of stoichiometric n-type MoS_2 is ~1.8 with sulfur vacancies, but this ratio increases up to 2.3 in p-type MoS_2 in which there are Mo vacancies or the sulfur level is enriched. Therefore, our samples have a slightly high S concentration. The more interesting result is that the Mo3$d_{5/2}$ and S2$p_{3/2}$ peaks are downshifted to almost the same extent when the thickness is increased from 2 to 12 layers, so the binding energy variation amounts to ~0.5 eV with a small broadening of ~0.1 eV, as indicated in Fig. 3(c). In order for the S2*p* binding energy to decrease, sulfur must be reduced further than the valence state of −2, which is much more unlikely to happen than variation in the Mo valence state.[37,38] Although the local presence of Mo metal with a ~1.2 eV lower binding energy was considered, as in the study of McDonnell *et al.*,[29] we found no evidence of n-doped sites in the CPD images nor are there peaks due to elemental Mo in the Mo3*d* spectra, so this effect is thought to be limited. Together with the absence of multiple Mo or S peaks, such as MoO_x or SO_x,[39] the similarity in the binding energy shifts implies an insignificant change in chemical bonding, if any. Since Mo metal was used as the growth source in the presence of H_2S gas instead of MoO_3, the occurrence of multiple oxidation states of residual MoO_x can also be excluded, as confirmed by the XPS data. Therefore, the peak downshifts can be assigned to hole-doping, since E_F, which represents zero energy, moves further away from the conduction band with hole-doping. Meanwhile, the presence of both water and adsorbed oxygen molecules is confirmed by Fig. 3(d): the series of O1*s* spectral envelopes for the films can be well fitted by the superposition of the three peaks located at 533.1, 532.4, and 531.4 eV, which are assigned to SiO_2, and adsorbed water and oxygen molecules, respectively.[35,40–42] Further, because SiO_2 was detected in the XP survey scan and the intensity of the SiO_2 peak decreased with increasing in the MoS_2 thickness, it is reasonable to attribute this peak at 533.1 eV to the SiO_2 substrate. Therefore, we conclude that the reason that the Mo3*d* and S2*p* binding energies decrease by similar amounts with increased numbers of layers is due to the weak bonding of oxygen or water molecules on the MoS_2 layers, which lowers the Fermi level of MoS_2.

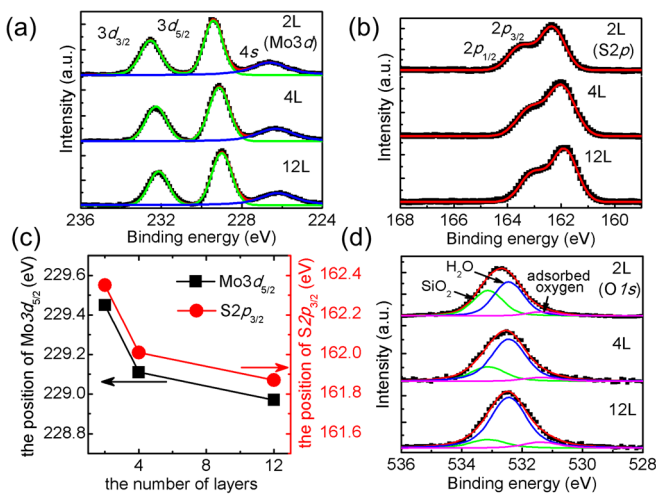

FIG. 3. (a) Mo3*d* and (b) S2*p* XPS curves for MoS_2 films with 2, 4, and 12 layers. (c) The peak positions of Mo3$d_{5/2}$ and S2$p_{3/2}$ as functions of thickness. As the films become thicker, there are negative shifts in both Mo3*d* and S2*p*, reflecting the p-doping effect. (d) O1*s* spectra for MoS_2 deconvoluted into the contributions of SiO_2, adsorbed O_2, and H_2O molecules.

In addition, PES experiments were conducted after heating the samples. We investigated the effects of molecular adsorption on the E_F of the 2- and 12-layer MoS_2 films before and after heating at 250 °C for 10 min. We used a photon energy of 650 eV for the survey scans of the core levels and 55.9 eV for the valence band. Energy calibration was carried out by measuring the distance between the Fermi edge of an Au film and the first harmonic. A voltage of −15 V was applied to each sample to accelerate electrons. Each work function can be easily evaluated with PES by measuring the width of the photoelectron spectrum and using the equation

$$\phi_{sample} = h\upsilon - (KE_{max} - KE_{min}), \quad (2)$$

where KE_{max} and KE_{min} are the maximum and minimum kinetic energies of the photoelectrons, which are determined from E_F and the secondary cut-off region, respectively. The photoelectron intensity for MoS_2 (filled symbols) is plotted as a function of kinetic energy with that of Au (blue line) in Fig. 4(a); the work function is determined from the threshold energy for electron emission. The data points for the 2- and 12-layer films are black and red, respectively, whereas the

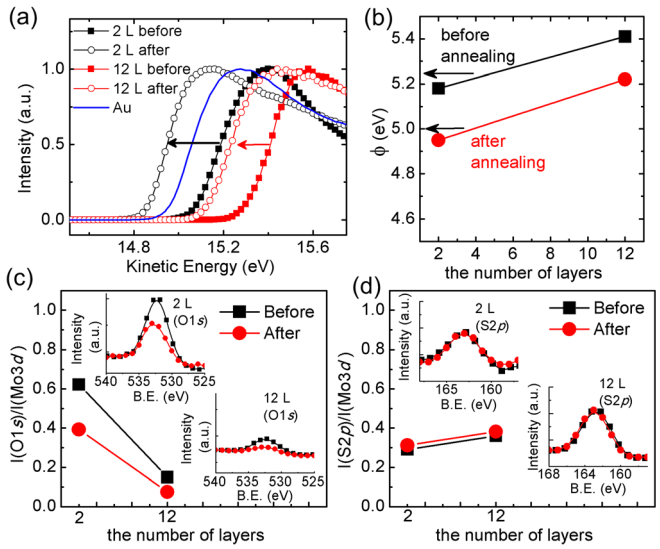

FIG. 4. (a) Secondary cut-off PES results for MoS_2 films with 2 and 12 layers. A gold film (blue line) was used as the reference, and its work function was determined to be 5.05 eV. The work function corresponds to the low energy cut-off position at half maximum. (b) The work functions of MoS_2 films with various thicknesses. The survey peak ratios for (c) O1s/Mo3d and (d) S2p/Mo3d before/after annealing are shown. The insets in (c) and (d) are the corresponding survey peak results normalized by the amplitude of the Mo3*d* peak.

filled and open symbols represent the pre- and post-annealed states, respectively. Based on Fig. 4(b), it is clear that the PES results reproduce the thickness dependence of the MoS_2 work function evident in the KFPM results. The PES results for the work function are lower than the KFPM results by ~50 mV, which arises because the surface state of Au is cleaner under UHV conditions than in the ambient environment.

Plotted as open symbols in Fig. 4(a), the post-annealed states of both samples have work functions that are remarkably reduced by ~0.2 eV. The survey scan is performed before and after annealing to confirm the changes of S, O, and Mo. After annealing, the intensities of the C1*s* peaks for adventitious carbon in the 2- and 12-layer MoS_2 films decreased by ~26 % and ~29 %, respectively. The peak ratios of O1*s*/Mo3*d* and S2*p*/Mo3*d* are plotted in Figs. 4(c) and 4(d), respectively. It can be seen that whereas the O1*s*/Mo3*d* ratio changed substantially as a result of annealing, S2*p*/Mo3*d* was largely unchanged for both the 2- and 12-layer films. The insets in Figs. 4(c) and 4(d) show the O1*s* and S2*p* peaks normalized by the Mo3*d* peak amplitude for each sample thickness as a function of the binding energy. Note that the inset scales are identical for the pre- and post-annealed 2- and 12-layer films and that the black and red symbols represent the pre- and post-annealed states, respectively. The removal of surface oxygen or water enhances the intensities of both the Mo and S peaks, so the ratio of O1*s* to Mo3*d* is increased by annealing in contrast to the ratio S2*p*/Mo3*d* for which almost no significant change is evident. Although the complete removal of adsorbed molecules is not expected to occur under such limited annealing conditions, this result indicates directly that the dominant contribution is from surface oxygen and H_2O and that such finite heating treatments can lower the work function of MoS_2 simply by removing adsorbed oxygen or water, not by inducing any Mo-deficient phase transformations.[43] According to Yue *et al.*,[31] the most suitable site for H_2O or O_2 adsorption is on top of a Mo atom; the corresponding charge transfer values are approximately 0.04 e and 0.01 e, respectively.

In conclusion, we have determined the work functions of CVD-grown MoS_2 films with various thicknesses on SiO_2. When the thickness increased from 2 to 12 layers, the work function was found to increase by ~0.2 eV in both the KPFM and PES results. The S and Mo core level shifts in the XPS results are similar, which implies the lowering of E_F due to physisorption variations rather than an altered chemical state; thus, these results originate from competing screening effects between the surface- and substrate-O_2/H_2O molecules. Our PES results show that the changed work function can be restored by removing such molecules with heating. The performance of MoS_2-based devices is controlled by an applied electric field, so this study provides insight into the variation with thickness of the charge transport and electrical properties of MoS_2 films.

This study was supported by IBS-R004-G4 and the Basic Science Research Program (2011-0014209) through a National Research Foundation of Korea grant funded by the Korean government Ministry of Science, ICT and Future Planning. C.C.H. acknowledges the support of the National Research Foundation of Korea (NRF) through the SRC Center for Topological Matter (No. 2011-0030787).

[1]Q. H. Wang, K. Kalantar-Zadeh, A. Kis, J. N. Coleman, and M. S. Strano, Nat. Nanotechnol. **7**, 699 (2012).
[2]B. Radisavljevic, A. Radenovic, J. Brivio, V. Giacometti, and A. Kis, Nat. Nanotechnol. **6**, 147 (2011).
[3]Y. J. Zhan, Z. Liu, S. Najmaei, P. M. Ajayan, and J. Lou, Small **8**, 966 (2012).
[4]M. R. Laskar, L. Ma, S. Kannappan, P. S. Park, S. Krishnamoorthy, D. N. Nath, W. Lu, Y. Y. Wu, and S. Rajan, Appl. Phys. Lett. **102**, 252108 (2013).
[5]Y. H. Lee, X. Q. Zhang, W. J. Zhang, M. T. Chang, C. T. Lin, K. D. Chang, Y. C. Yu, J. T. W. Wang, C. S. Chang, L. J. Li, and T. W. Lin, Adv. Mater. **24**, 2320 (2012).
[6]Y. F. Yu, C. Li, Y. Liu, L. Q. Su, Y. Zhang, and L. Y. Cao, Sci. Rep. **3**, 1866 (2013).
[7]Y. Lee, J. Lee, H. Bark, I. K. Oh, G. H. Ryu, Z. Lee, H. Kim, J. H. Cho, J. H. Ahn, and C. Lee, Nanoscale **6**, 2821 (2014).
[8]H. S. Lee, S. W. Min, Y. G. Chang, M. K. Park, T. Nam, H. Kim, J. H. Kim, S. Ryu, and S. Im, Nano Lett **12**, 3695 (2012).
[9]S. Kim, A. Konar, W. S. Hwang, J. H. Lee, J. Lee, J. Yang, C. Jung, H. Kim, J. B. Yoo, J. Y. Choi, Y. W. Jin, S. Y. Lee, D. Jena, W. Choi, and K. Kim, Nat. Commun. **3**, 1011 (2012).
[10]T. Jin, J. Kang, E. S. Kim, S. Lee, and C. Lee, J. Appl. Phys. **114**, 164509 (2013).
[11]J. Feng, X. F. Qian, C. W. Huang, and J. Li, Nat. Photonics **6**, 866 (2012).
[12]T. Mori, T. Kozawa, T. Ohwaki, Y. Taga, S. Nagai, S. Yamasaki, S. Asami, N. Shibata, and M. Koike, Appl. Phys. Lett. **69**, 3537 (1996).
[13]H. C. Diaz, R. Addou, and M. Batzill, Nanoscale **6**, 1071 (2014).
[14]J. Y. Park, S. Kwon, and J. H. Kim, Adv. Mater. Interfaces **1**, 1300089 (2014).
[15]A. Molina-Sanchez and L. Wirtz, Phys. Rev. B **84**, 155413 (2011).
[16]C. Lee, H. Yan, L. E. Brus, T. F. Heinz, J. Hone, and S. Ryu, ACS Nano **4**, 2695 (2010).
[17]H. Li, Q. Zhang, C. C. R. Yap, B. K. Tay, T. H. T. Edwin, A. Olivier, and D. Baillargeat, Adv. Funct. Mater. **22**, 1385 (2012).
[18]R. Wang, S. N. Wang, D. D. Zhang, Z. J. Li, Y. Fang, and X. H. Qiu, ACS Nano **5**, 408 (2011).
[19]J. H. Kim, J. H. Hwang, J. Suh, S. Tongay, S. Kwon, C. C. Hwang, J. Q. Wu, and J. Y. Park, Appl. Phys. Lett. **103**, 171604 (2013).

[20]J. Y. Cheon, J. H. Kim, J. H. Kim, K. C. Goddeti, J. Y. Park, and S. H. Joo, J. Am. Chem. Soc. **136**, 8875 (2014).
[21]S. McDonnell, A. Azcatl, R. Addou, C. Gong, C. Battaglia, S. Chuang, K. Cho, A. Javey, and R. M. Wallace, ACS Nano **8**, 6265 (2014).
[22]R. Fivaz and E. Mooser, Phys. Rev. **163**, 743 (1967).
[23]A. Ayari, E. Cobas, O. Ogundadegbe, and M. S. Fuhrer, J. Appl. Phys. **101**, 014507 (2007).
[24]H. Li, Z. Y. Yin, Q. Y. He, H. Li, X. Huang, G. Lu, D. W. H. Fam, A. I. Y. Tok, Q. Zhang, and H. Zhang, Small **8**, 63 (2012).
[25]Y. Li, C. Y. Xu, B. Y. Zhang, and L. Zhen, Appl. Phys. Lett. **103**, 033122 (2013).
[26]M. Fontana, T. Deppe, A. K. Boyd, M. Rinzan, A. Y. Liu, M. Paranjape, and P. Barbara, Sci. Rep. **3**, 1634 (2013).
[27]Z. Y. Zeng, Z. Y. Yin, X. Huang, H. Li, Q. Y. He, G. Lu, F. Boey, and H. Zhang, Angew. Chem. Int. Ed. **50**, 11093 (2011).
[28]K. Dolui, I. Rungger, and S. Sanvito, Phys. Rev. B **87**, 165402 (2013).
[29]S. McDonnell, R. Addou, C. Buie, R. M. Wallace, and C. L. Hinkle, ACS Nano **8**, 2880 (2014).
[30]W. Zhou, X. L. Zou, S. Najmaei, Z. Liu, Y. M. Shi, J. Kong, J. Lou, P. M. Ajayan, B. I. Yakobson, and J. C. Idrobo, Nano Lett. **13**, 2615 (2013).
[31]Q. Yue, Z. Z. Shao, S. L. Chang, and J. B. Li, Nanoscale Res. Lett. **8**, 425 (2013).
[32]S. Das and J. Appenzeller, Phys. Status Solidi-R **7**, 268 (2013).
[33]S. Das, H. Y. Chen, A. V. Penumatcha, and J. Appenzeller, Nano Lett. **13**, 100 (2013).
[34]D. J. Late, B. Liu, H. S. S. R. Matte, V. P. Dravid, and C. N. R. Rao, ACS Nano **6**, 5635 (2012).
[35]H. Qiu, L. J. Pan, Z. N. Yao, J. J. Li, Y. Shi, and X. R. Wang, Appl. Phys. Lett. **100**, 123104 (2012).
[36]C. D. Wagner and G. E. Muilenberg, *Handbook of X-ray Photoelectron Spectroscopy* (Perkin-Elmer, 1979).
[37]M. A. Baker, R. Gilmore, C. Lenardi, and W. Gissler, Appl. Surf. Sci. **150**, 255 (1999).
[38]J. R. Lince, D. J. Carre, and P. D. Fleischauer, Langmuir **2**, 805 (1986).
[39]A. Azcatl, S. McDonnell, K. C. Santosh, X. Peng, H. Dong, X. Y. Qin, R. Addou, G. I. Mordi, N. Lu, J. Kim, M. J. Kim, K. Cho, and R. M. Wallace, Appl. Phys. Lett. **104**, 111601 (2014).
[40]J. A. Taylor, G. M. Lancaster, A. Ignatiev, and J. W. Rabalais, J. Chem. Phys. **68**, 1776 (1978).
[41]J. W. He, X. Xu, J. S. Corneille, and D. W. Goodman, Surf. Sci. **279**, 119 (1992).
[42]G. T. Kim, T. K. Park, H. S. Chung, Y. T. Kim, M. H. Kwon, and J. G. Choi, Appl. Surf. Sci. **152**, 35 (1999).
[43]H. W. Wang, P. Skeldon, and G. E. Thompson, J. Mater. Sci. **33**, 3079 (1998).